Implementation of Adaptive Neuro-Fuzzy Inference System Control on Pneumatic Solar Tracker

Baisrum Baisrum[1] Budi Setiadi[1,*] Sudrajat Sudrajat[1] Varian Wijayakusuma[1] Hilmi Ulhaq[1] Rina Hikmawati[1] Naufal Qamaruddin[1] Sandi Hardiansyah[1]

[1] *Department of Electrical Engineering, Politeknik Negeri Bandung, Indonesia*
[*]*Corresponding author. Email: budi.setiadi@polban.ac.id*

ABSTRACT
The use of servo/stepper motor actuators in solar tracker systems requires additional gear components. These additional components affect the movement response output of the solar tracker system. This study research the accuracy, response output of a single-axis solar tracker system using pneumatic actuators and ultraviolet (UV) sensors. The type of pneumatic actuator used is a double-acting cylinder. The pneumatic actuator functions to move the solar tracker mechanically and are connected directly to the solar panel frame. Solar tracker moves from east to west automatically and vice versa. The movement of the solar tracker angle from 0^0 to 45^0 based on the combined reading of 2 UV sensors (UVx and UVy). The direction of movement of the tracker is regulated through 4 digital valves which are operated digitally. While the tracker speed is regulated through 1 proportional valve which is operated continuously. The opening and closing of the digital valve and the size of the proportional valve opening are regulated based on the results of the data processing and signal conditioning on the microcontroller. The data processing method uses an adaptive neuro-fuzzy inference system (ANFIS). The ANFIS architecture uses a Sugeno fuzzy model with 2 inputs and 9 rules. Changes in the ANFIS output value are based on the combined reading feedback input from the UV sensor. System testing was carried out with a UV lamp. The experimental results show an average error of 1.6^0 for no-load conditions and 2.5^0 for loaded conditions in the east-west direction. The dynamic response of the system produces 2.08% overshoot, and 1.25% steady-state error.

Keywords: *Solar Tracker, Double-Acting Cylinder, Valve, ANFIS, UV Sensor.*

1. INTRODUCTION

Solar power plants are included in the category of new renewable energy power plants. Movable solar panels based on actuators integrated with solar trackers. The position of the maximum angle of sunlight cannot be predicted based on changes in time and calendar [3]-[7]. To get a good angle position, the solar panels mounted on the solar tracker can be moved automatically, continuously/discretely. The integration of servo motor actuators and solar trackers has an impact on the direction of rotational and translational motion following the capture of sunlight. Changes in the direction of motion of the solar tracker are based on sensor feedback (optical combination sun, UV, photodiode, infrared, LDR) [4]-[6], [7], [9], [10], [12], [13]. The solar tracker can be driven automatically with long time range changes. The prediction of angle changes is based on forecasting weather conditions using the deep learning method [6].

The position of the solar tracker rotates 3 times a day (morning, afternoon, and evening) [3]. The use of servo/stepper motors as actuators in one-axis or two-axis solar trackers has shortcomings in terms of response and the addition of gear components to the system [3], [4], [6]-[13]. The use of fuzzy on one-axis solar-tracker with UV sensor as feedback produces slow response movement output. The impact of the reflected light effect on the sensor [5].

This research designs and prototypes a hybrid system is integrating pneumatic actuators and electronic control systems. It is expected to get good accuracy, dynamic response results because the actuator is mechanically connected directly to the solar panel frame. The control method used is ANFIS 2 inputs and

9 rules. ANFIS input is obtained from the combined reading feedback of 2 UV sensors embedded on the east and west sides of the solar panel.

2. BACKGROUND

Referring to the hybrid control research, the pneumatic system is superior. Pneumatic actuators produce large torque, small physical, easy installation, avoid sparks due to electrical hazards, and better kinematics than electric actuators [1], [2], [5], [11].

The research testing was carried out in a laboratory room in daytime conditions. The test was carried out using a UV lamp as a substitute for sunlight. The use of UV lamps was based on the similarity of the characteristics of sunlight.

Previous research discusses solar trackers using servo/stepper motor actuators. Actuators with additional gear components are used to automatically move the solar panel frame based on feedback from the LDR sensor [12], [13]. Feedback from the optical combination sun sensor [4]. And without using sensors, the system works based on the division of time (morning, afternoon, and evening) [3]. Meanwhile, other research discusses hybrid solar trackers, a combination of pneumatic actuators and electronic controls. The data processing on the electronic control uses the fuzzy method [5].

3. RESEARCH METHODS

This research is divided into two parts, namely hardware, and software. The result of this research is the realization of a system tested on a laboratory scale.

3.1. Hardware

The hardware consists of electronic and pneumatic parts. Electronics functions to process data from sensor feedback, and the result is a signal that is forwarded to pneumatics.

3.1.1 Electronic Design

Figure 1 shows the overall electronic block diagram design. The electronic block consists of input, process, signal processing, and output.

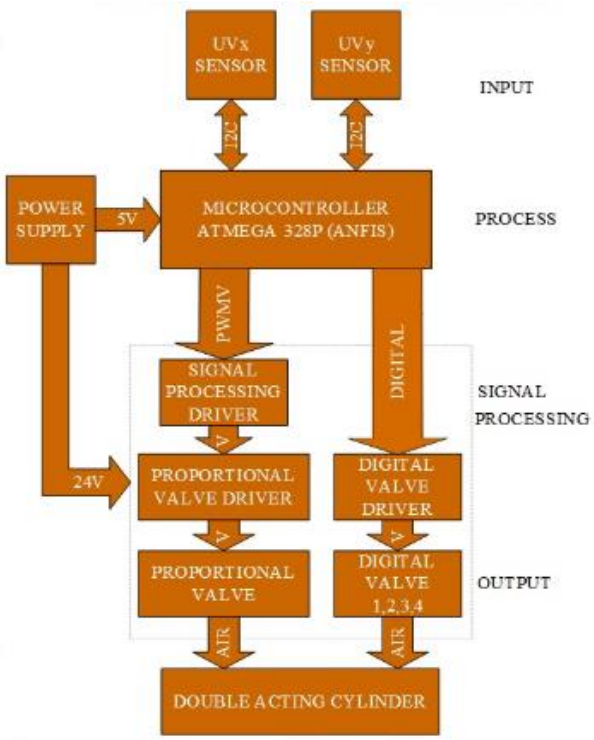

Figure 1 Electronic Block Diagram

The input block consists of two UV sensors (x and y) with I2C communication. UVx is placed on the east side and UVy on the west side of the solar panel. Both UV sensors function to read the value of UV radiation from the sun. The result of reading the UV index value serves as a dynamic setpoint value and feedback for data processing in the microcontroller. The process block uses the Arduino platform ATMega328P microcontroller. The microcontroller serves to process the incoming data from the UV sensor readings.

Furthermore, it is processed using the ANFIS algorithm and produces 2 output signals: digital and pulse width modulation (PWM). The signal processing block consists of proportional and digital driver blocks. The signal processing driver (h-bridge-type L293D) functions to process the signal PWM to voltage (V) with a range of 0-5 volts. Then the V signal is flowed to the proportional driver (VEA 250), and is converted into a V signal with the current limit setting automatically. The digital driver (h-bridge-type L298N) converts digital logic signals into V by amplifying the current. The output block consists of digital and proportional valve actuators. The digital valve serves to regulate the direction of airflow through the double-acting cylinder. The proportional valve functions to regulate the speed of airflow through the double-acting cylinder.

Table 1 shows the specifications of electronic use.

Table 1. Electronic Specifications

No	Component	Specification/Type
1	VEML6070	UV Sensor, I2C, 2.7-5.5, UV Index, Infrared Index
2	Microcontroller	ATMega328P, Arduino UNO, Arduino Nano Platform
3	L298N	Double H-Bridge, max 32 Vdc/ 5 A
4	L293D	Double H-Bridge, max 32 Vdc/ 1 A
5	VEA 250	Voltage Source 24Vdc, Input Voltage 0-5V
6	Power Supply	24 Vdc/10A, 5Vdc/2A
7	UV Lamp	220Vac/25 Watt

3.1.2 Pneumatic Design

Figure 2 shows a block diagram of the pneumatic. The system design consists of a cylinder double acting as a solar tracker actuator, 4 digital valves, 1 proportional valve, air service unit, and compressor.

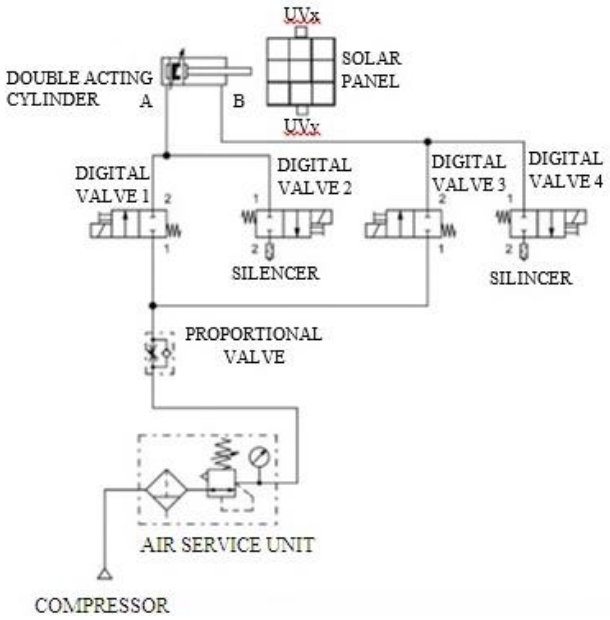

Figure 2 Pneumatic Block Diagram

The compressor produces air which serves as an energy source for all pneumatic components (double-acting cylinders, proportional and digital valves). Air from the compressor is supplied to the air service unit. The air service unit has three functions: filtering water droplets contained in the air, distributing oil lubrication, and regulating pressure. Furthermore, the energy source that has been processed in the air service unit is channeled to the double-acting cylinder through proportional and digital valves. The proportional valve functions to regulate the speed of airflow through the double-acting cylinder. The digital valve serves to regulate the direction of airflow through the double-acting cylinder (A→B or B→A).

Table 2 shows an overview of the speed and direction of airflow through the double-acting cylinder. Mode number 1, the condition of the airflow direction is from A to B or east to west on digital valves (1, 4) ON and digital valves (2, 3) OFF. Mode number 2, the condition of the airflow direction is from B to A or west to east on digital valves (1, 4) OFF and digital valves (2, 3) ON. Meanwhile, the speed response of the solar tracker is influenced by the percentage of proportional valve openings between 0.1 till 25%. Mode number 3, the airflow condition is compressed so that the double-acting cylinder stops. All digital valves are in the OFF state, and the proportional valve opening percentage is 0%.

Table 3 shows the specifications of the pneumatic used.

Table 2. Description of the Direction of Movement of Airflow

No	Digital Valve 1	Digital Valve 2	Digital Valve 3	Digital Valve 4	PROPORTIONAL VALVE OPENING PERCENTAGE (%)	DOUBLE-ACTING CYLINDER (AIRFLOW)	MOVEMENT OF SOLAR TRACKER
1	ON	OFF	OFF	ON	0.1 s/d 25	A → B	East to West
2	OFF	ON	ON	OFF	0.1 s/d 25	B → A	West to East
3	OFF	OFF	OFF	OFF	0	Stop	Stop

Table 3. Pneumatic Specifications

No	Component	Specification/Type
1	Compressor	Voltage Source 220 Vac, silent, 3/4 hp
2	Air Service Unit	Lubricant, Regulator, Oil, max 10 bar, Hose 8 mm
3	Proportional Valve	One Way, 1/8, 0,7 Mpa, Voltage Analog 24 Vdc / 4 Watt, Hose 6 mm
4	Digital Valve	2/2, Spring, Coil 24 Vdc, Hose 6 mm
5	Double Acting Cylinder	Stroke 250 mm, tube Ø 25 mm, Hose 6 mm
6	Silencer	1/4", BSL-02

3.2. Software

Figure 3 shows the ANFIS architecture with 2 inputs and 9 rules. The input variable x contains the UV index value of the UVx sensor. The input variable y contains the UV index value of the UVy sensor.

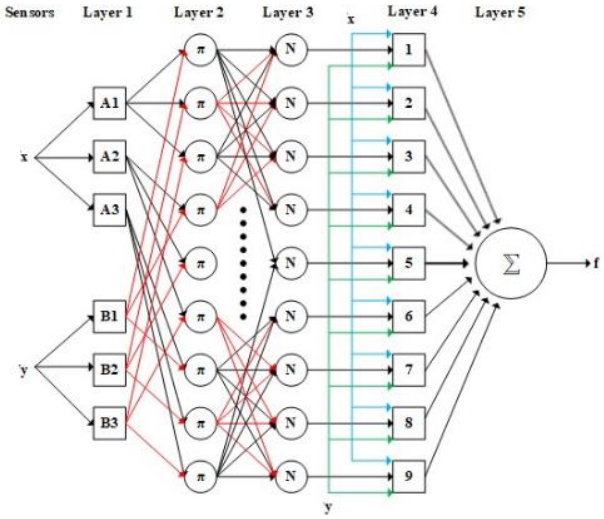

Figure 3 ANFIS Architecture

ANFIS rules are formed based on the if-then model of Takagi and Sugeno, which can be stated as follows:

Rule 1: if x is A_1 and y is B_1
Rule 2: if x is A_1 and y is B_2
Rule 3: if x is A_1 and y is B_3
Rule 4: if x is A_2 and y is B_1
Rule 5: if x is A_2 and y is B_2
Rule 6: if x is A_2 and y is B_3
Rule 7: if x is A_3 and y is B_1
Rule 8: if x is A_3 and y is B_2
Rule 9: if x is A_3 and y is B_3

The description of ANFIS layers is given below:

Layer 1: consists of 2 variables, A and B. Each variable consists of 3 nodes (A_1, A_2, A_3) and (B_1, B_2, B_3). Each node represents a linguistic label (A_1 =low, A_2 =moderate, A_3 =high, B_1 =low, B_2=moderate, B_3=high). The linguistic function uses a bell membership function (MF) with a range of UV index values of low (0-3), moderate (2-6.5), and high (5-7). Each node of this layer is adaptive, and the output is given by:

$$\theta_{1,i} = \mu A_i(x), \quad for\ i = 1,2,3 \tag{1}$$
$$\theta_{1,i-3} = \mu B_{i-3}(y), \quad for\ i = 4,5,6 \tag{2}$$

Where x (or y) is the input to node i and A_i (or B_{i-3}) is the linguistic label (such as "low," "moderate," or "high") associated with this node. In other words, $\theta_{1,i}$ is the degree of membership of the fuzzy set A (= A_1, A_2, A_3, B_1, B_2 or B_3) and represents the degree to which input x (or y) satisfies quantifier A. The following membership function for A from bell linguistics:

$$\mu A_i(x) = \frac{1}{1+\left|\frac{x-c_i}{a_i}\right|^{2b_i}} \tag{3}$$

Layer 2: The nodes are fixed nodes denoted as Π. The outputs of this layer can be symbolized as.

$$\theta_{2,i} = w_i = \mu A_1(x)\mu B_i(y), \quad for\ i = 1,2,3 \tag{4}$$
$$\theta_{2,i+3} = w_{i+3} = \mu A_2(x)\mu B_i(y), for\ i = 1,2,3 \tag{5}$$
$$\theta_{2,i+6} = w_{i+6} = \mu A_3(x)\mu B_i(y), for\ i = 1,2,3 \tag{6}$$

Layer 3: The nodes are too fixed. They are labeled N, indicating that they play a normalization role to the firing strengths from the preceding layer. The output from the i[th] node is the normalized firing strength given by:

$$\theta_{3,i} = \overline{w_i} = \frac{w_i}{w_1+w_2+\ldots+w_9}, for\ i = 1,2,\ldots,9 \quad (7)$$

Layer 4: The nodes are adaptive. The output of each node in this layer is simply the product of the normalized firing strength and a first-order polynomial. Thus, the outputs of this layer are given by:

$$\theta_{4,i} = \overline{w_i} fi = \overline{w_i}(p_i x + q_i y + r_i) \quad (8)$$
$$for\ i = 1,2,\ldots,9$$

(p_i, q_i, r_i) is the parameter set of this node, referred to as consequent parameters.

Layer 5: This node performs the summation of all entering signals. There is only a single fixed node labeled Σ. The general output of the model is given by:

$$\theta_{5,i} = \sum_i \overline{w_i} fi = \frac{\sum_i w_i f_i}{\sum_i w_i}, \quad for\ i = 1,2,\ldots 9 \quad (9)$$

3.3. System Realization

Figure 4 shows the electro-pneumatic realization for the solar tracker system. The solar tracker is built by integrating pneumatic mechanics and electronic control devices.

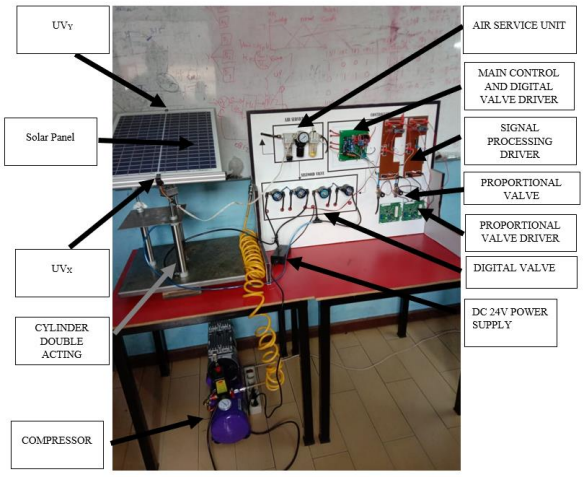

Figure 4 System Realization

3.4. Testing

Testing of the solar tracker system was carried out using a UV lamp. The angle of light that enters the UV sensor is varied from 0^0 to 45^0 in 5^0 increments, as shown in Figure 5. The test stage consists of 3 (UV sensor, direction angle, and response). Meanwhile, the goals of the research test results are in the form of an average directional error and the dynamic response of the system.

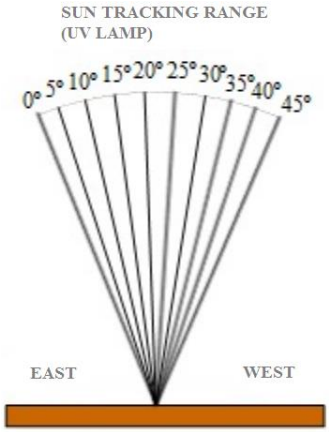

Figure 5 Sun Tracking Range (UV Lamp)

3.4.1. UV Sensor

UV sensor testing is carried out to see the functionality of each sensor reading, accuracy comparison, and system dynamic setpoint values. The test was carried out with a mechanical load of 50Wp (4000 gr) solar panel. The distance between the sensor and the UV lamp was set at 25cm. Figure 6 and Figure 7 show the results of sensor readings. The graph of the readings of the two sensors shows an average UV index value of 2.4. The comparison of reading accuracy is close, so the two components are feasible to be used simultaneously.

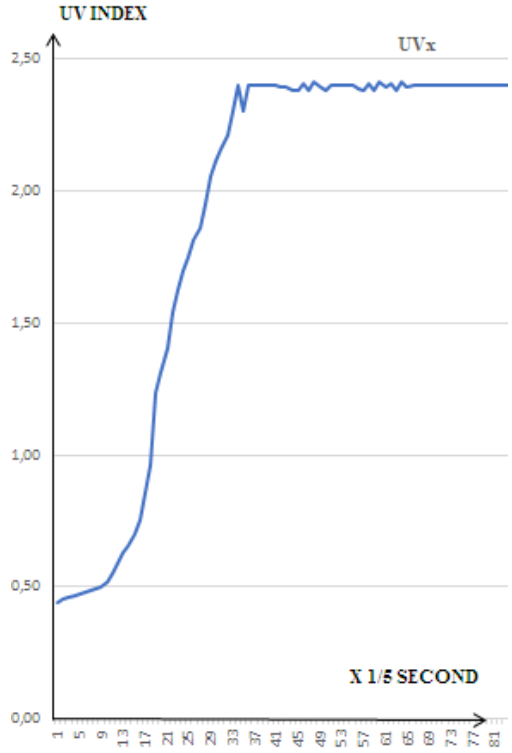

Figure 6 UVx Sensor Test Results

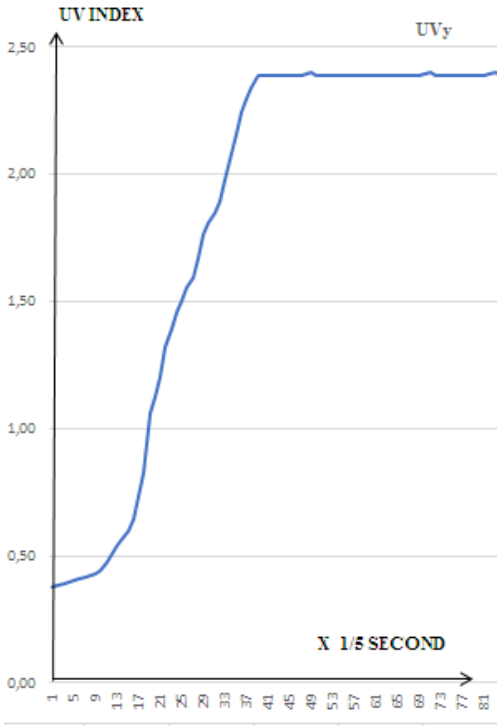

Figure 7 UVy Sensor Test Results

Figure 8 shows the results of testing the two UV sensors simultaneously. In the initial conditions of the test, the position of the solar tracker is at an angle of 0^0 and the UV lamp at an angle of 22.5^0. The UV lamp distance is set at 25cm. The solar tracker moves automatically and stops when the difference in sensor readings (Uvx and UVy) is close to zero (error ± 0.1). One of the final values of the sensor readings is used as a dynamic setpoint value.

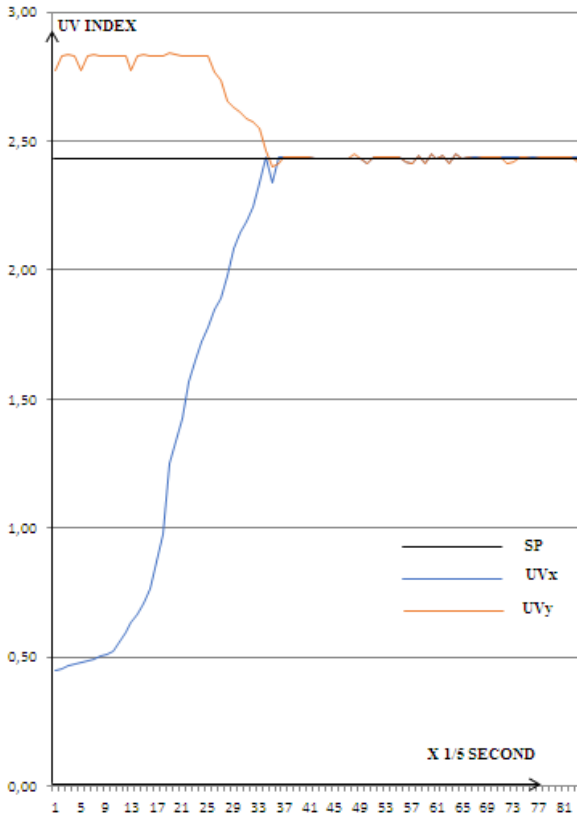

Figure 8 Dynamic SetPoint

3.4.2. Angle Direction

Table 4 shows an overview of the angle of UV light to the position of the solar tracker. The UV light beam starts from east to west with a variation of the angle increment every 5^0. The test was carried out with 2 conditions, no-load and 50Wp (4000g) solar panel load.

Table 4. Angle At The East to West Direction

UV Light Beam Angle (º)	The Angle Of The Solar Tracker (º)		Error (º)	
	Without Load	Solar Panel Load (4000gr)	Without Load	Solar Panel Load (4000gr)
0	0	0	0	0
5	5	5	0	0
10	10	10	0	0
15	16	15	1	0
20	20	21	0	1
25	24	27	1	2
30	31	31	1	1
35	35	36	0	1
40	39	41	1	1
45	45	45	0	0
Error Average (º)			1.6	2.5

3.4.3.Dynamic Response

Figure 8 shows a graph of the dynamic response of the solar tracker system test. The test was carried out on a laboratory scale with artificial UV lighting. The dynamic setpoint (SP) obtained is 2.40 INDEX. The SP value is obtained automatically from the comparison between the UVx and UVy sensors so that the difference is close to zero.

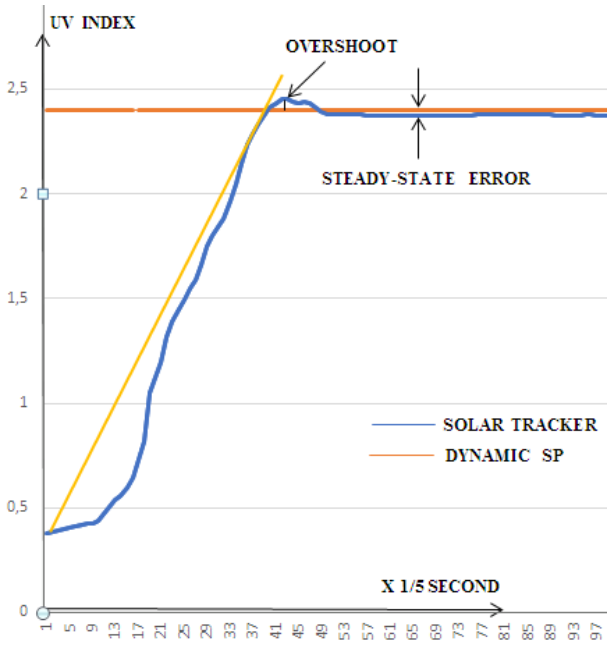

Figure 9 Solar Tracker System Dynamic Response

The test results obtained the value of steady-state error and overshoot. The data is recorded directly from the microcontroller to an excel export file. The following is the process of analyzing the calculation.

a. Steady-state error is obtained:

$$Steady\ State\ Error = \frac{(2.43-2.40)}{2.40}\ x\ 100\% = 1.25\%$$

b. Maximum Overshoot is the highest value from the graph is 2.45 then:

$$Overshoot = \frac{(2.45-2.40)}{2.40}\ x\ 100\% = 2.08\%$$

The test data showed a better dynamic response than previous studies [5].

4. CONCLUSION

The use of the ANFIS method to automate electro-pneumatic solar trackers has been successfully designed and implemented. The results of laboratory-scale experiments show that the system can track the direction of sunlight with an error of 1.6^0 for no-load conditions and 2.5^0 for loaded conditions in the east-west direction. And it produces a dynamic response of 2.08% overshoot and 1.25% steady-state error.

ACKNOWLEDGMENTS

The research team would like to thank P3M Politeknik Negeri Bandung for research funding through the Penelitian Peningkatan Kapasitas Laboratorium (PPKL) scheme with decree number B/74.4/PL1.R7/PG.00.03/2021

REFERENCES

[1] S. Mori, K. Tanaka, S. Nishikawa, R. Niiyama, Y. Kuniyoshi, High-Speed Humanoid Robot Arm for Badminton Using Pneumatic-Electric Hybrid Actuators, IEEE Robotics and Automation Letters, 2019, pp. 1-8. DOI: 10.1109/LRA.2019.2928778

[2] S. Hirzel, ET. AL, Electric or Pneumatic? Comparing Electric and Pneumatic Linear Drives with Regard to Energy Efficiency and Costs, ECEEE Industrial Summer Study Proceedings, pp.475-485. 2014.

[3] A. Smirnov, A. G. Vozmilov, P. A.Romanov, Comparison of Discrete Sun Tracking Methods for Photovoltaic Panels, International Conference on Industrial Engineering, Applications and Manufacturing (ICIEAM), Sochi, Russia, 2019, pp. 1-5.

[4] A. Díaz, R. Garrido**,** J. J. Soto-Bernal, A Filtered Sun Sensor for Solar Tracking in HCPV and CSP Systems, in IEEE Sensors Journal, **2019,** pp. 917-925.

[5] **B.** Baisrum, B. Setiadi, S. W. Jadmiko, Sudrajat, V. A. Wijayakusuma, F. Z. Raihan, Solar Tracker Elektro-Pneumatik Berbasis Kendali Fuzzy, Rekayasa Hijau: Jurnal Teknologi Ramah Lingkungan, **2020**, pp. 179-190**.DOI**: https://doi.org/10.26760/jrh.v4i3.179-190

[6] C. Kasburg, S. Frizzo Stefenon, Deep Learning for Photovoltaic Generation Forecast in Active Solar Trackers, in IEEE Latin America Transactions, 2019, pp. 2013-2019. DOI: 10.1109/TLA.2019.9011546.

[7] C. D. Rodríguez-Gallegos, O. Gandhi, S. K. Panda, T. Reindl, On the PV Tracker Performance: Tracking the Sun Versus Tracking the Best Orientation, in IEEE Journal of Photovoltaics, 2020, pp. 1474-1480. DOI: 10.1109/JPHOTOV.2020.3006994.

[8] H. Fathabadi, Novel Online Sensorless Dual-Axis Sun Tracker, in IEEE/ASME Transactions on Mechatronics, 2017, pp. 321-328. DOI: 10.1109/TMECH.2016.2611564.

[9] J. Wu, X. Chen, L. Wang, Design and Dynamics of a Novel Solar Tracker With Parallel Mechanism, in IEEE/ASME Transactions on Mechatronics, 2016, pp. 88-97. DOI: 10.1109/TMECH.2015.2446994.

[10] T. Kamal, M. Karabacak, S. Z. Hassan, H. Li, L. M. Fernández-Ramírez, A Robust Online Adaptive B-Spline MPPT Control of Three-Phase Grid-Coupled Photovoltaic Systems Under Real Partial Shading Condition, in IEEE Transactions on Energy Conversion, 2019, pp. 202-210. DOI: 10.1109/TEC.2018.2878358.

[11] Z. Lin, T. Zhang, Q. Xie, Q. Wei, Intelligent Electro-Pneumatic Position Tracking System Using Improved Mode-Switching Sliding Control With Fuzzy Nonlinear Gain, in IEEE Access, 2018, pp. 34462-34476.

[12] P. Rani, O. Singh, and S. Pandey, An Analysis on Arduino-based Single Axis Solar Tracker, in 5th IEEE Uttar Pradesh Section International Conference on Electrical, Electronics and Computer Engineering (UPCON), 2018, pp. 1–5. Doi: 10.1109/UPCON.2018.8596874.

[13] S. Hawibowo, I. Ala, R. B. Citra Lestari, and F. R. Saputri, Stepper Motor Driven Solar Tracker System for Solar Panel, in 4th International Conference on Science and Technology (ICST), Yogyakarta, 2018, pp. 1–4. Doi: 10.1109/ICSTC.2018.8528571.

[14] H. Abu-Rub, A. Iqbal, Sk. Moin Ahmed, F. Z. Peng, Y. Li, and G. Baoming, Quasi-Z-Source Inverter-Based Photovoltaic Generation System With Maximum Power Tracking Control Using ANFIS, IEEE Trans. Sustain. Energy, 2013, pp. 11–20. Doi: 10.1109/TSTE.2012.2196059.